PHYSICAL REVIEW E **79**, 010201(R) (2009)

Ion structure in warm dense matter: Benchmarking solutions of hypernetted-chain equations by first-principle simulations

K. Wünsch, J. Vorberger, and D. O. Gericke
Centre for Fusion, Space and Astrophysics, Department of Physics, University of Warwick, Coventry CV4 7AL, United Kingdom
(Received 7 November 2008; published 6 January 2009)

We investigate the microscopic structure of strongly coupled ions in warm dense matter using *ab initio* simulations and hypernetted chain (HNC) equations. We demonstrate that an approximate treatment of quantum effects by weak pseudopotentials fails to describe the highly degenerate electrons in warm dense matter correctly. However, one-component HNC calculations for the ions agree well with first-principles simulations if a linearly screened Coulomb potential is used. These HNC results can be further improved by adding a short-range repulsion that accounts for bound electrons. Examples are given for recently studied light elements, lithium and beryllium, and for aluminum where the extra short-range repulsion is essential.

DOI: 10.1103/PhysRevE.79.010201 PACS number(s): 61.20.−p, 52.27.Gr, 52.65.−y, 67.10.Hk

I. INTRODUCTION

The structural properties of warm dense matter (WDM) provide the basis for a general understanding of such diverse systems as giant gas planets [1,2], laser-heated solids, and imploding capsules of hydrogen during inertial confinement fusion [3]. The availability of intense lasers makes it nowadays possible to investigate WDM in the laboratory by x-ray scattering [4–7]. The interpretation of the x-ray scattering signal and its application as diagnostics need, however, theoretical input for the structural properties of WDM. Such a model should be fast and simple enough to allow for a similar treatment as developed for weakly coupled plasmas [8]. A fitting routine based on hypernetted chain (HNC) equations seems applicable; however, a validation of such approximate results by means of first-principles simulations is required.

The theoretical investigation of WDM is challenging since it requires a consistent description of interacting systems with degenerate electrons and strongly coupled ions. Here, we will discuss two approaches: the classical HNC method based on integral equations developed in fluid theory and first-principles simulations using density functional molecular dynamics (DFT MD). For purely classical systems, the first approach is known to yield reasonably accurate results, but the quantum nature of the electrons can only be treated approximately. Nevertheless, this method provides high numerical efficiency. In contrast, *ab initio* simulations like DFT MD aim to describe fully interacting quantum systems. That is, they include strong ionic correlations as well as the quantum behavior for the electrons. This treatment exactly meets the requirements of WDM, but such simulations demand much computing power.

We investigate the ionic structure in simple elements for parameters recently studied [4,7]. The goal is to benchmark the HNC approach by DFT-MD simulations and, thereby, investigate the applicability of often used effective interaction potentials. In particular, pseudopotentials designed to incorporate quantum effects in classical approaches are tested. Once the effective ion-ion potential is understood, the ion structure in WDM can be determined very efficiently by the HNC approach.

II. METHODS

The spatial arrangement of the particles in WDM can be described by the pair distribution function $g_{ab}(r)$ or the static structure factor $S_{ab}(k)$. These functions are connected via Fourier transformation. For multicomponent isotropic systems, we have [9]

$$S_{ab}(k) = \delta_{ab} + \frac{4\pi\sqrt{n_a n_b}}{k}\int_0^\infty dr\, r^2[g_{ab}(r) - 1]\sin(kr). \quad (1)$$

First, we briefly discuss the classical HNC approach. This method combines the Ornstein-Zernike and the HNC closure relations [10–12]

$$h_{ab}(\mathbf{r}) = c_{ab}(\mathbf{r}) + \sum_c n_c \int d\bar{\mathbf{r}} c_{ac}(\bar{\mathbf{r}}) h_{cb}(|\mathbf{r} - \bar{\mathbf{r}}|), \quad (2)$$

$$g_{ab}(\mathbf{r}) = \exp[-\beta V_{ab}(\mathbf{r}) + h_{ab}(\mathbf{r}) - c_{ab}(\mathbf{r})]. \quad (3)$$

This system of coupled integral equations can be solved numerically for an arbitrary number of components [13]. The bridge diagrams neglected in the HNC approximation (3) are well known to be of minor importance for the intermediate coupling strengths considered here.

Here, we use two versions of the HNC approach. The first one considers only the ions explicitly, and the electrons are treated either as a uniform, neutralizing background [one-component plasma (OCP) model] or as a polarizable background (Yukawa model). In the latter case, linear screening leads the Yukawa or Debye potential

$$V_{ii}^{Y}(r) = \frac{Z^2 e^2}{r}\exp(-\kappa r) \quad (4)$$

as an effective ion-ion interaction. Of course, the OCP limit is recaptured for $\kappa=0$. The Yukawa (Y) model treats the electrons within linear response which is applicable as long as the electron-ion interaction is weak. To describe the partially degenerate electrons in WDM, the inverse screening length κ should be calculated by $\kappa^2=(4e^2 m_e/\pi\hbar^3)\int dp f_e(p)$ with the Fermi distribution $f_e(p)$. The classical Debye-Hückel law and Thomas-Fermi screening are included as limiting cases.

Second, we use a multicomponent version of the HNC equations to consider both electrons and ions on equal footing which also goes beyond linear screening. To include quantum effects inherent for electrons, pseudopotentials must be applied for the electron-ion and electron-electron interactions. In this way, quantum diffraction and exchange can be treated approximately within classical methods. In this paper, we consider a simple form of the Klimontovich-Kraeft (KK) potential [14] and, for one example, the Deutsch potential [15]. For WDM conditions, both potentials are much weaker than the Coulomb potential. A more detailed comparison with other quantum pseudopotentials can be found in Ref. [13].

The approximate descriptions of electron-ion systems presented above should be compared to first-principles quantum simulations. Here, we use DFT MD as available in the VASP code [16–18]. It relies on the Born-Oppenheimer approximation to decouple the ionic and electronic degrees of freedom. For every MD step, the Kohn-Sham equations [19] are self-consistently solved for the electronic ground state in the external field of the ions. This ground state is defined on the basis of the Mermin functional to incorporate temperature effects on the electron distribution [20]. The electronic exchange-correlation contribution is estimated via the generalized gradient approximation (GGA) [21]. The electron-ion interaction is modeled using the projector augmented-wave (PAW) method [22,23], which makes it possible to include all electrons (core and valence) into the calculations in an efficient manner. Finally, Hellmann-Feynman forces can be derived from the electronic wave functions to move the ions with classical Newton dynamics.

The electron wave functions are represented by plane waves with an energy cutoff of 300 eV (Al) and 800 eV (Be, Li), respectively. In the calculations for beryllium and lithium, all electrons are treated as valence electrons. For aluminum, the full inner shells were treated as core states. The Brillouin zone was sampled at the Γ point only. The high temperatures (compared to solids) of the WDM state require a substantial number of electronic bands to properly represent the tail of the Fermi distribution.

The MD part of the simulations uses a time step of 0.192 fs and up to 2000 MD steps after equilibration. Simulations were performed with 108–250 ions whose temperature was controlled by a Nose-Hoover thermostat [24].

III. RESULTS AND DISCUSSION

The presented comparison of results from the HNC and DFT-MD calculations are an attempt (i) to find the HNC version that matches the DFT-MD simulations best and (ii) to indirectly obtain information about the effective ion-ion interactions. The WDM states chosen for analysis in this paper are very similar to those created in recent experiments [4,5,7,25].

Figure 1 considers warm dense beryllium under several compression levels. Independent of the density, the ion charge state can be estimated to be close to $Z=2$. The two-component HNC calculations for electron-ion systems use the Klimontovich-Kraeft potential (labeled HNC-KK). Such

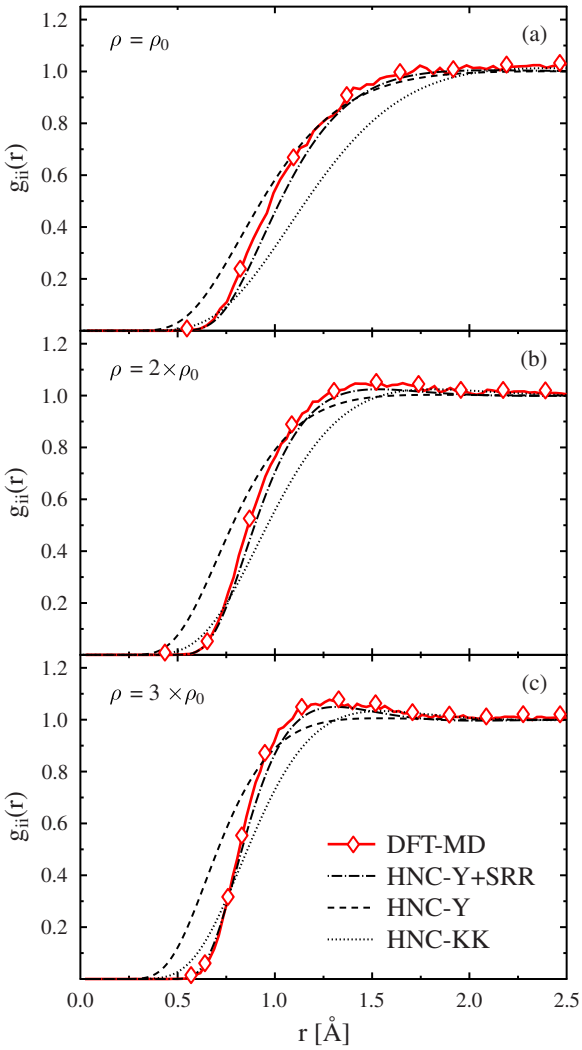

FIG. 1. (Color online) Ion-ion pair distribution functions $g_{ii}(r)$ in warm dense beryllium at multiples of the normal density $\rho_0 = 1.848$ g/cm^3: (a) normal density, (b) $\rho=2\rho_0$ (2 times compressed), and (c) $\rho=3\rho_0$. The temperature and the ion charge state (for HNC) are $T=13$ eV and $Z=2$, respectively.

a treatment results in pair distributions that rise less sharply, but are shifted to the right. This is generally the case when the ions are coupled too strongly or are less effectively screened. Although screening is self-consistently described within the two-component HNC approach, the use of the KK potential with very soft electron-ion interactions leads to strongly reduced screening clouds around the ions. The ions, in turn, interact more strongly. Indeed, the resulting pair distributions are very close to OCP results (not shown) for all cases.

Surprisingly, the model, which considers only ions that interact via screened Coulomb forces (labeled HNC-Y), works rather well when compared to the DFT-MD data. In particular, larger distances and the shoulder of the pair distribution in the upper two panels of Fig. 1 are nicely described. This fact indicates that screening can be considered to be linear for larger distances.

Large discrepancies arise for small distances where the ion-ion repulsion appears to be underestimated by the HNC

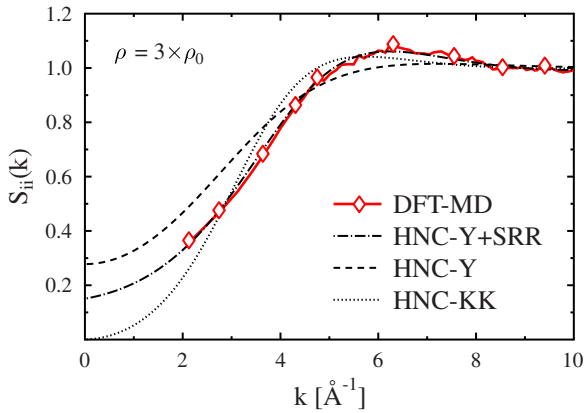

FIG. 2. (Color online) Static ion-ion structure factor $S_{ii}(k)$ for compressed beryllium under conditions as in Fig. 1(c).

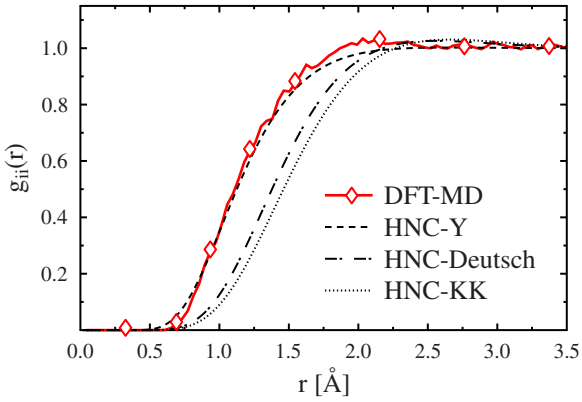

FIG. 3. (Color online) Ion-ion pair distribution of lithium with $T=5$ eV, $\rho=0.85$ g/cm^3, and $Z=1.6$.

approaches discussed so far. They can be understood on the basis of the electronic configuration of the beryllium ions with $Z\sim 2$. Regardless of temperature and compression, the ions still have an intact $1s^2$ shell. When these shells start to overlap, an additional repulsive force arises due to the Pauli exclusion principle. The forbidden overlap of the electron orbitals can be modeled by an additional short-range repulsion (SRR)

$$V_{ii}^{\mathrm{Y+SRR}}(r) = \frac{a}{r^4} + \frac{Z^2e^2}{r}\exp(-\kappa r). \tag{5}$$

The power in the SRR was obtained from a fit to the potentials directly extracted from the simulations [26]. The parameter a is related to the radial extension of the ion and defines the strength of the short-range repulsion. Here, it is used to fit the pair distributions, but it is kept constant for the same material under all conditions; it would only change due to further ionization.

The potential (5), labeled Y+SRR, gives the desired larger correlation hole in the pair distributions when used in the HNC approach. In particular, for the highly compressed beryllium in Fig. 1(c), the additional repulsion is significant to reproduce the correct interparticle spacing and the maximum in the distribution.

Figure 2 shows the static ion-ion structure factor related to the case in Fig. 1(c). Again, the KK potential leads to a OCP-like behavior—i.e., $S_{ii}(0)\approx 0$. The application of other pseudopotentials (not shown) yields results between HNC-KK and HNC-Y. They show, however, not the same shape as the DFT-MD results. As for the pair distributions, the best agreement with the DFT-MD data can be obtained by the use of a Yukawa potential with an additional short-range repulsion (Y+SRR). The structure factor from DFT MD is restricted to k values larger than $2\pi/L$ where L is the length of the simulation box. Therefore, HNC is a valuable tool to calculate the structure factor for smaller values. The results should be considered with caution though since algebraic screening known to occur for large distances [27,28] is not incorporated.

As a second example, the ionic structure of warm dense lithium is studied. Comparisons as in Fig. 3 were used to extract the ion charge state from the DFT-MD data which was then combined with inelastic x-ray scattering for diagnostics of a shocked sample [7]. Once more, the KK potential and also the Deutsch potential (labeled HNC-Deutsch) fail to describe screening correctly. In contrast, the Yukawa model yields good agreement with DFT-MD simulations over the whole range. An additional short-range repulsion is here not required since the higher ionization destroys the full $1s$ shell.

Warm aluminum is discussed in the last example of Fig. 4. Under these conditions, the ions are strongly coupled ($\Gamma \approx 170$) and the pair distribution shows its typical characteristics: well-pronounced maxima and a large correlation hole. Results similar to the DFT-MD data, but slightly shifted to larger r, are achieved by the HNC approach for an OCP. The overestimated second maximum indicates, however, that screening is important here, although HNC calculations using linear screening (4) show by far not enough spatial correlations.

One should, however, keep in mind that aluminum ions possess full inner shells under these conditions. As for beryllium, these bound electrons lead to an additional repulsion between the ions at short distances. After taking this SRR into account, the ion-ion pair distribution obtained by HNC also shows the typical characteristics for a strongly coupled system and agrees well with the simulation data. Interest-

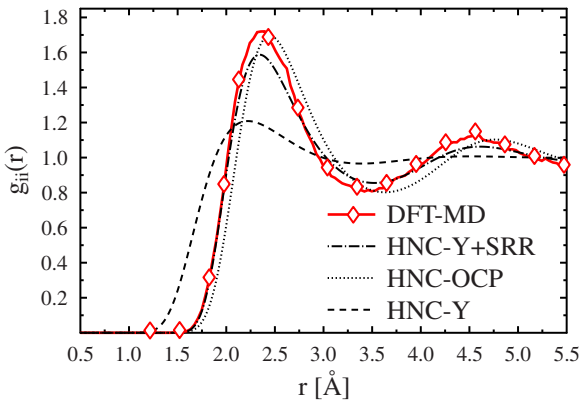

FIG. 4. (Color online) Ion-ion pair distribution for aluminum with $T=1.1$ eV, $\rho=3.4$ g/cm^3, and $Z=3$.

ingly, these correlations are here not due to strong Coulomb forces as in highly ionized dense plasmas, but due to the interaction of full inner shells. In other words, these ionic correlations mainly result from the Pauli principle applied to shells of bound electrons.

IV. CONCLUSIONS

We investigated the ion structure in warm dense matter applying the classical HNC approach and *ab initio* quantum simulations. The comparisons for different systems show that effective potentials, which mimic quantum effects in multicomponent HNC calculations, do not yield agreement with the quantum simulations. Although the Klimontovich-Kraeft potential is an extreme case, this fact holds for other quantum potentials as well.

A simple linearly screened Coulomb potential used in HNC calculations for the ions only is, however, often in good agreement with the DFT-MD results. The results can be considerably improved by including additional short-range repulsion due to the forbidden overlap of bound electrons in full shells. It has been shown that an appropriate algebraic potential can mimic this effect.

In conclusion, the Yukawa potential with an additional short-range repulsion can describe the ionic structure of WDM in agreement with the results from the DFT-MD simulations even for ions with many bound electrons.

ACKNOWLEDGMENTS

We gratefully acknowledge financial support from the U.K. Engineering and Physical Sciences Research Council.

[1] T. Guillot *et al.*, in *Jupiter*, edited by W. M. F. Bagenal *et al.* (Cambridge University Press, Cambridge, England, 2004).
[2] B. Militzer, W. B. Hubbard, J. Vorberger, I. Tamblyn, and S. A. Bonev, Astrophys. J. Lett. **688**, L45 (2008).
[3] J. D. Lindl *et al.*, Phys. Plasmas **11**, 339 (2004).
[4] S. H. Glenzer, G. Gregori, R. W. Lee, F. J. Rogers, S. W. Pollaine, and O. L. Landen, Phys. Rev. Lett. **90**, 175002 (2003).
[5] S. H. Glenzer *et al.*, Phys. Rev. Lett. **98**, 065002 (2007).
[6] A. L. Kritcher *et al.*, Science **322**, 69 (2008).
[7] E. García Saiz *et al.*, Nat. Phys. **4**, 940 (2008).
[8] G. Gregori, S. H. Glenzer, W. Rozmus, R. W. Lee, and O. L. Landen, Phys. Rev. E **67**, 026412 (2003).
[9] J. P. Hansen and I. R. McDonald, *Theory of Simple Liquids* (Academic, London, 1990).
[10] J. M. J. van Leeuwen, J. Groeneveld, and J. de Boer, Physica (Amsterdam) **25**, 792 (1959).
[11] J. DeBoer, J. M. J. Van Leeuwen, and J. Groeneveld, Physica (Amsterdam) **30**, 2265 (1964).
[12] L. Ornstein and F. Zernike, Proc. R. Acad. Sci. Amsterdam **17**, 793 (1914).
[13] K. Wünsch, P. Hilse, M. Schlanges, and D. O. Gericke, Phys. Rev. E **77**, 056404 (2008).
[14] Y. Klimontovich and W.-D. Kraeft, High Temp. Phys. (USSR) **12**, 212 (1974).
[15] C. Deutsch, Phys. Lett. **60A**, 317 (1977).
[16] G. Kresse and J. Hafner, Phys. Rev. B **47**, 558 (1993).
[17] G. Kresse and J. Hafner, Phys. Rev. B **49**, 14251 (1994).
[18] G. Kresse and J. Furthmüller, Phys. Rev. B **54**, 11169 (1996).
[19] W. Kohn and L. J. Sham, Phys. Rev. **140**, A1133 (1965).
[20] N. D. Mermin, Phys. Rev. **137**, A1441 (1965).
[21] J. P. Perdew, K. Burke, and M. Ernzerhof, Phys. Rev. Lett. **77**, 3865 (1996).
[22] P. E. Blöchl, Phys. Rev. B **50**, 17953 (1994).
[23] G. Kresse and D. Joubert, Phys. Rev. B **59**, 1758 (1999).
[24] W. G. Hoover, Phys. Rev. A **31**, 1695 (1985).
[25] E. García Saiz, G. Gregori, F. Y. Khattak, J. Kohanoff, S. Sahoo, G. Shabbir Naz, S. Bandyopadhyay, M. Notley, R. L. Weber and D. Riley, Phys. Rev. Lett. **101**, 075003 (2008).
[26] S. Izvekov, M. Parinello, C. J. Burnham, and G. A. Voth, J. Chem. Phys. **120**, 10896 (2004).
[27] A. Alastuey and Ph. A. Martin, Phys. Rev. A **40**, 6485 (1989).
[28] R. Kjellander, J. Phys. A **39**, 4631 (2006).